

Accepted Manuscript

On the intermolecular interaction of N-benzylquininium chloride or quinine with some carbonyl group containing compounds

Thais C. Avila, Marcelo M. Reginato, Cláudio Di Vitta, Lucas C. Ducati, Leandro H. Andrade, Liliana Marzorati

PII: S0040-4039(16)30338-0
DOI: <http://dx.doi.org/10.1016/j.tetlet.2016.03.109>
Reference: TETL 47497

To appear in: *Tetrahedron Letters*

Received Date: 1 March 2016
Revised Date: 28 March 2016
Accepted Date: 31 March 2016



Please cite this article as: Avila, T.C., Reginato, M.M., Vitta, C.D., Ducati, L.C., Andrade, L.H., Marzorati, L., On the intermolecular interaction of N-benzylquininium chloride or quinine with some carbonyl group containing compounds, *Tetrahedron Letters* (2016), doi: <http://dx.doi.org/10.1016/j.tetlet.2016.03.109>

This is a PDF file of an unedited manuscript that has been accepted for publication. As a service to our customers we are providing this early version of the manuscript. The manuscript will undergo copyediting, typesetting, and review of the resulting proof before it is published in its final form. Please note that during the production process errors may be discovered which could affect the content, and all legal disclaimers that apply to the journal pertain.

On the intermolecular interaction of N-benzylquininium chloride or quinine with some carbonyl group containing compounds.

Thais C. Avila, Marcelo M. Reginato, Cláudio Di Vitta, Lucas C. Ducati, Leandro H. Andrade, Liliana Marzorati*

Instituto de Química, Universidade de São Paulo, P.O. Box 26077 005513-970, Av. Prof. Lineu Prestes 748, São Paulo, S.P., Brazil

*Corresponding Author E-mail: lmazora@iq.usp.br.

ABSTRACT

Interactions between N-benzylquininium chloride (Quibec) and some carbonyl group containing compounds were investigated using ^1H NMR and theoretical calculations. Results highlight the importance of the hydrogen bonding between the Quibec C-9 hydroxyl group and the carbonyl oxygen in addition to π - π stacking between the carbonyl acceptor and the alkaloid donor.

Keywords: chiral discrimination; Quibec; quinine; ^1H NMR;

Introduction

One of the most challenging topics in modern chemistry refers to the understanding of the origin of molecular recognition between chiral organocatalysts and achiral substrates with all related consequences for the achievement of successful asymmetric transformations.¹⁻³ On the other hand, the determination of enantiomeric excesses rely on the ability of a wide range of chiral discriminating agents to generate diastereomeric associated pairs. In both cases,

NMR^{4,5} and computational methods^{6,7} are powerful tools to access the mutual orientation of the molecular partners.

In our laboratory, while dealing with chiral phase-transfer catalysts, we became interested in investigating *N*-benzylquininium chloride (Quibec; **1**; Figure 1) as a promoter of enantiodifferentiation in CDCl₃ solution, at room or low temperature, using ¹H NMR spectroscopy. It should be mentioned that although the mechanism of asymmetric induction by **1** or structurally related alkaloid salts in enolate based reactions seems to be well established,^{8,9} their potential for chiral molecular recognition of neutral species was less explored.^{10,11} In this sense, when phosphoryl- or carbamoylquinines¹²⁻¹⁴ were used as chiral discriminating agents, the existence of a free unhindered quinuclidine nitrogen seemed to guarantee the enantioselection of acidic-type substrates. However, **1**, devoid of such basic site for interaction, has been reported¹⁵ to provide very similar stereochemical environments for two enantiomeric alcohols.

On the other hand, the increased acidity of C-9 hydroxyl group of **1**, as a result of the quaternization of the quinuclidine nitrogen, could allow for an efficient hydrogen bonding to the basic carbonyl oxygen of carbonyl or of some carboxylic acid derivatives. On the basis of this reasoning, we decided to investigate the capability of **1**, as compared to quinine, to induce ¹H NMR nonequivalence of enantiotopic nuclei pertaining to the same molecule or to discriminate between two enantiomeric solutes. To this end, compounds **2** - **6** (Figure 1) were prepared and submitted to ¹H NMR analysis as mixtures of increasing donor/acceptor molar ratios.

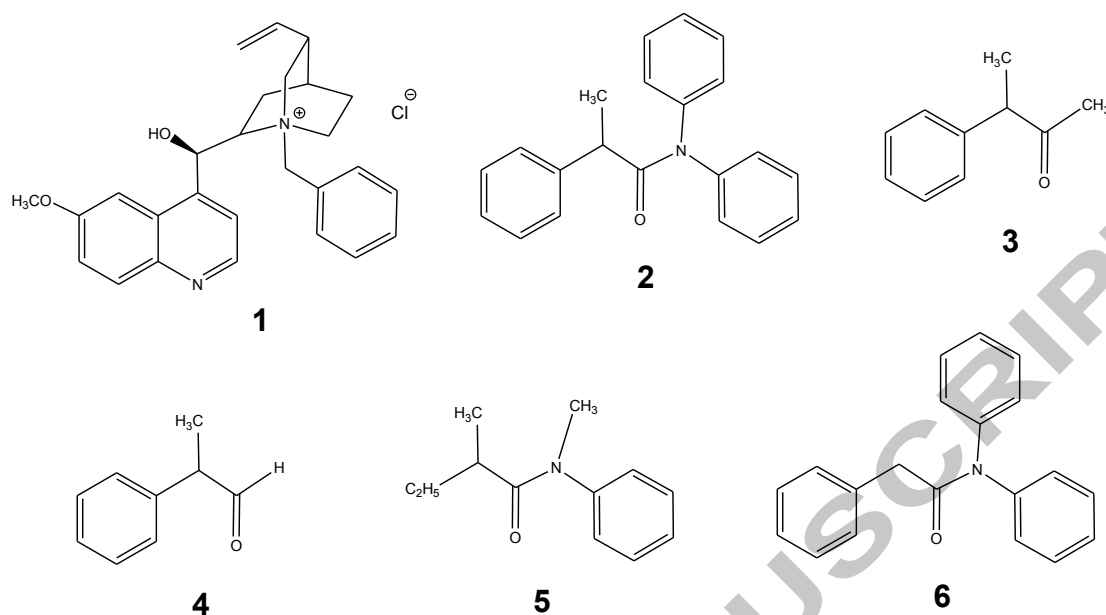


Figure 1. Compounds of this work.

Results and Discussion

In the case of mixtures of **1** with amide **2**, progressive resolution of the signal for the methyl group into two superimposed doublets was observed by increasing the donor/acceptor molar ratio. Better results were obtained at $-20\text{ }^{\circ}\text{C}$, in line with the expectation of a tighter interacting system (Figure 2). It should be mentioned that the molar ratio **1** : substrate could not be extended beyond 2.5, due to the solubility constraints. Although the $\Delta\Delta\delta$ values showed a linear increase with increasing molar ratio, upfield shift ($\Delta\delta$) was more pronounced for one of the two enantiomers (see Figure 2 in which symbols ■ and ● refer to the enantiomers of **2**).

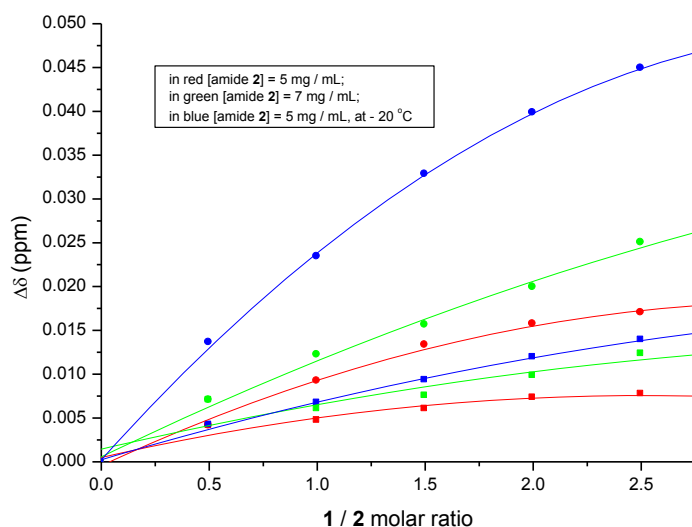


Figure 2. $\Delta\delta$ versus 1 / 2 molar ratio.

Aiming to identify the enantiomer that better fitted solvation, we decided to prepare enantiomerically pure **2**, starting from (*R*)-phenylpropionic acid, readily transformed into the corresponding acid chloride to be submitted to reaction with sodium diphenylamide. In order to ascertain enantiomeric purity, the ^1H NMR spectrum of the newly prepared (*R*)-**2** was recorded in admixture with **1**, at a molar ratio of 2.0 (**1** / amide). As can be seen in Figure 3, no racemization occurred during the preparation process, and the *R* configuration could be unequivocally assigned to the enantiomer resonating at lower frequency.

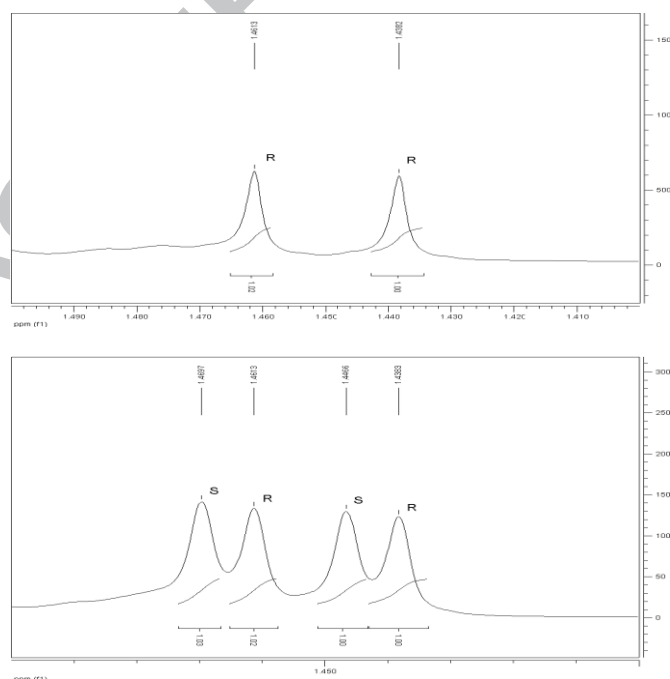


Figure 3. Comparative ^1H NMR spectra for the methyl signals of mixtures of (a) **1** / pure (*R*)-**2** and (b) **1** / (+)-**2**.

Surprisingly, for compound **3**, no signal separation could be seen at room temperature, even at the molar ratio of 2.5. At a lower temperature, the doublets were less resolved as compared to compound **2**. This result could be attributed either to the differential polarization of the carbonyl groups in both compounds or to the presence of extra phenyl groups in compound **2** favoring π -stacking with the aromatic rings of **1**.

Having in hand the above set of results, we decided to investigate the origin of the chiral recognition phenomenon observed for the diastereomeric pairs of **1** / **2**.

The geometrical optimizations of **1** and **2** were performed at the DFT-B97D3/cc-pVDZ level of theory with Gaussian 09 package of program.¹⁶ In order to include dispersion and hydrogen bonding effects, Grimme's D3 corrections were also considered.¹⁷ Six different conformations for each amide enantiomer, resulting from variation of the dihedral angle H-C-C=O, and the optimized conformation of the chiral discriminator were assembled into 24 pairs, in which the additive (**1**) was placed to the left or to the right sides of the amide molecule, favoring the larger number of intermolecular interactions. Figure 4 shows two examples of such pairs, for which the hydrogen bond (amide C=O / C-9 OH group of **1**) and π -stacking interactions are highlighted in black and red, respectively.

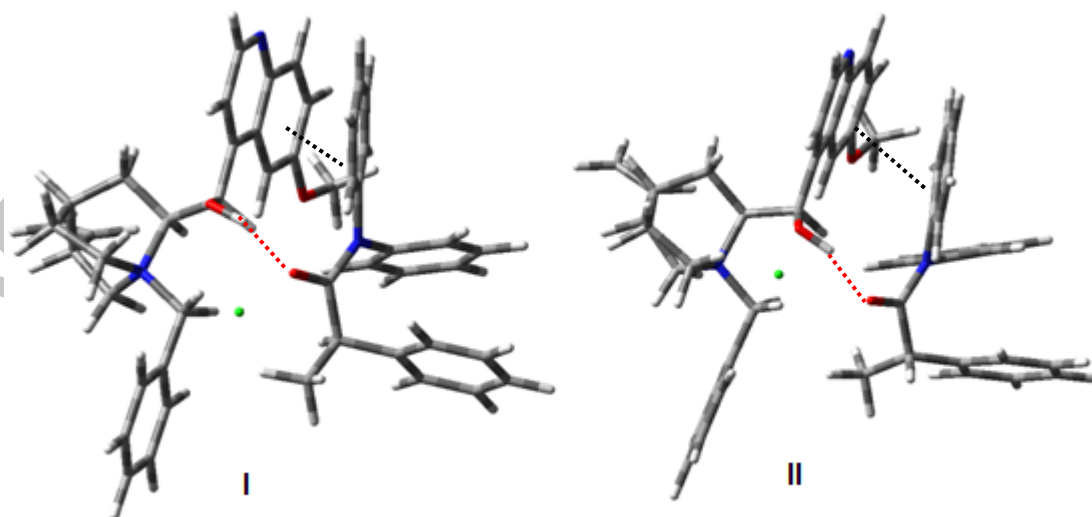


Figure 4. **1** / substrate pairs for: (I) (*R*)-**2**; (II) (*S*)-**2** (optimized at B97D3/cc-pVDZ level of theory) for **1** placed to the left of **2**, considering the green dot as the chloride ion.

As for the (*R*)-enantiomer the relative energies of the 12 pairs for which **1** is placed either to the right or to the left sides are shown in Table 1. Analogously, the relative energies for the 12 pairs of the (*S*)-enantiomer are reported in Table 2.

Table 1.

Relative energies (kcal mol⁻¹) for the arrangements of **1** placed to the left (column A) or to the right (column B) sides of several conformations of (*R*)-**2** optimized at B97D3/cc-pVDZ level of theory. The relative energies in respect to global most stable conformer are shown in parentheses.

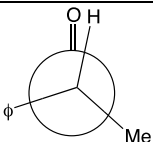
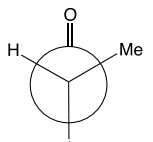
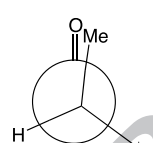
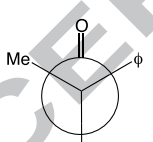
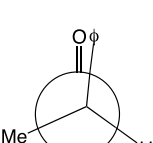
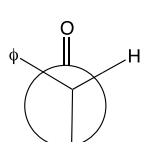
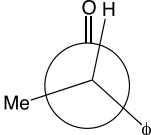
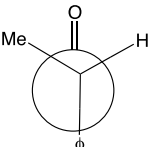
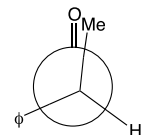
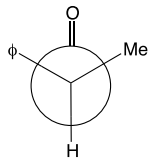
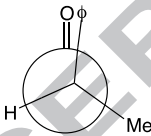
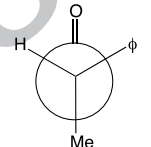
entry	Conformation	A		B	
		E a.u.	ΔE kcal.mol ⁻¹	E a.u.	ΔE kcal.mol ⁻¹
1		-2708.14945	4.18 (4.18)	-2708.14650	3.95 (6.03)
2		-2708.14945	4.18 (4.18)	-2708.14903	2.36 (4.44)
3		-2708.15611	0.00 (0.00)	-2708.14896	2.40 (4.49)
4		converged to the most stable conformer for this arrangement		converged to the most stable conformer for this arrangement	
5		-2708.15369	1.51 (1.51)	-2708.15279	0.00 (2.08)
6		-2708.14750	5.40 (5.40)	-2708.146006	4.25 (6.34)

Table 2.

Relative energies (kcal mol⁻¹) for the arrangements of **1** placed to the left (column C) or to the right (column D) sides of several conformations of (*S*)-**2** optimized at B97D3/cc-pVDZ level of theory. The relative energies in respect to global most stable conformer are shown in parentheses.

entry	Conformation	C		D	
		E a.u.	ΔE kcal.mol ⁻¹	E a.u.	ΔE kcal.mol ⁻¹
1		converged to the fourth most stable conformer for this arrangement		-2708.14657	5.80 (5.80)
2		-2708.15115	2.17 (2.93)	-2708.14657	5.80 (5.80)
3		-2708.15388	0.45 (1.22)	-2708.15582	0.00 (0.00)
4		-2708.15281	1.13 (1.89)	converged to the most stable conformer for this arrangement	
5		-2708.15461	0.00 (0.76)	converged to the most stable conformer for this arrangement	
6		converged to the most stable conformer for this arrangement		converged to the second most stable conformer for this arrangement	

Considering the global most stable arrangements of the (*R*)-enantiomer with **1** placed to its left side (entry 3-column A) or to its right side (entry 5-column B), the relative energy difference is 2.08 kcal.mol⁻¹ in favor of that in entry 3-column A (Table 1).

On the other hand, according to Table 2, for the (*S*)-enantiomer, the global most stable arrangements are those in entry 3-column D and in entry 5-column C. The relative energy difference is 0.76 kcal.mol⁻¹ in favor of this first arrangement.

For both arrangements (entry 3-column A (Table 1) and entry 3-column D (Table 2)) the steric repulsion between the phenyl group linked to the stereogenic center and **1** overcomes any possible stabilization by π -stacking. Although at B97D3/cc-pVDZ level of theory there is no preference between these two arrangements (only 0.18 kcal.mol⁻¹ in favor of (*R*)-**2** / **1** arrangement), after their re-optimization, including PCM solvent effects (CDCl₃), at B97D3/cc-pVTZ level of theory¹⁸ (and using counterpoise corrections¹⁹), the energy difference became $\Delta E = 2.12$ kcal.mol⁻¹ and $\Delta G = 2.37$ kcal.mol⁻¹ in favor of that of entry 3-column D (Table 2).

Considering the two most stable arrangements, the upfield shift of the ¹H NMR doublet for both enantiomers can be explained by the anisotropic effect of the aromatic ring of **1** on the methyl group of **2**. However, it should be noted that for the pair with the (*R*)-enantiomer (at the left side in Figure 6) the methyl group is better positioned towards the shielding region of the aromatic ring as compared to the pair with the (*S*)-enantiomer (at the right side in Figure 5). Furthermore, a stronger interaction between aromatic rings for the (*R*)-enantiomer as compared to the (*S*)-isomer (quinoline-phenyl vs phenyl-phenyl) is expected. In fact, the counterpoise calculations for these two arrangements are -32.88 and -30.46 kcal mol⁻¹, respectively, amounting to a difference of 2.42 kcal mol⁻¹. Therefore, the better quinoline-phenyl interaction seems to be responsible for the higher stabilization for the arrangement shown in entry 3-column A (Table 1) leading to a higher $\Delta\delta$ value for the **1** / (*R*)-**2** diastereomeric pair. Theoretical ¹H chemical shift calculations at IEFPCM(CDCl₃)-B3LYP/cc-pVTZ level of theory corroborates this assumption as the δ values for the methyl groups of **2** in arrangements shown in entry 3-column A (Table 1) and in entry 3-column D (Table 2), are 0.7 ppm and 1.0 ppm, respectively.

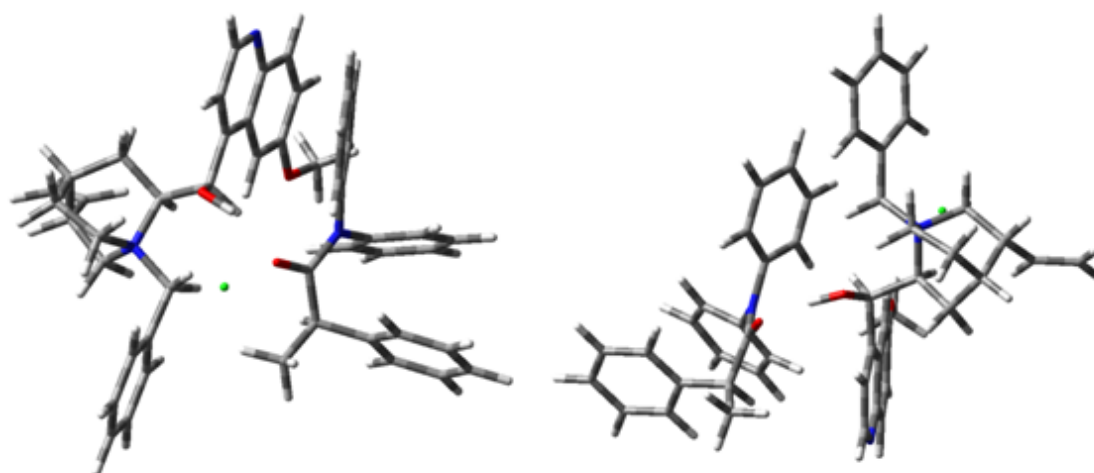


Figure 5. The most stable pairs at IEFPCM-B97D3/cc-pVTZ level of theory, considering the green dot as the chloride ion.

In a set of similar experiments, the ^1H NMR spectra of mixtures of **1** and compounds **3** or **4** were recorded. Figures 6 and 7 (in which symbols \blacksquare and \bullet refer to the enantiomers of each compound) present the experimental $\Delta\delta$ vs **1** / substrate molar ratios for these compounds at two different temperatures.

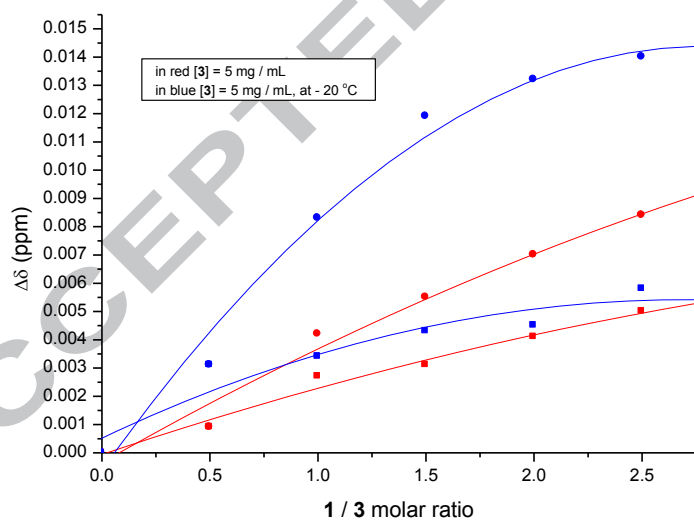


Figure 6. $\Delta\delta$ versus **1** / **3** molar ratio.

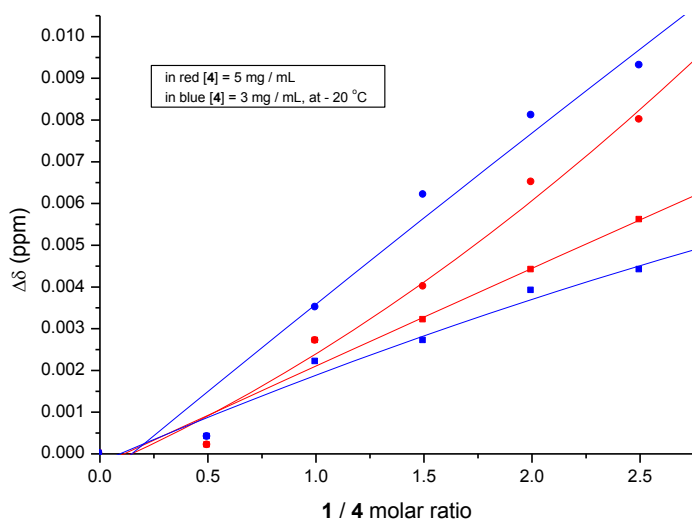


Figure 7. $\Delta\delta$ versus 1 / 4 molar ratio.

For both carbonyl compounds **3** and **4** lower $\Delta\delta$ values were observed as compared to those for compound **2** (Figures 2, 6 and 7). This seems to be in line with the expected basicity order: amide > aldehyde > ketone. Additionally, for compounds **3** and **4**, lower $\Delta\Delta\delta$ values were also observed (Table 3).

Table 3.

$\Delta\Delta\delta$ values for mixtures of **1** and substrates **2** - **4** (5 mg / mL), at the 2.5 : 1 (**1** : substrate) molar ratio.

Compound	$\Delta\Delta\delta$ (ppm)	
	(r. t.)	(-20 °C)
2	0.0092 (0.0126)*	0.0310
3	0.0033	0.0083
4	0.0024	0.0049**

* substrate concentration: 7 mg / mL

** substrate concentration: 3 mg / mL

The comparison of spectral data for racemic **3** and of pure (*R*)-3-phenyl-2-butanone (prepared from (*R*)-phenylpropanoic acid and 2 mol equivalents of methyl lithium) allowed for the assignment of *R* configuration to the ketone isomer for which the corresponding solvate resonates at a lower frequency.

In order to test the importance of the α -phenyl moiety as a promoter of interaction with **1**, analogous experiments were performed with 2-methylundecanal. In fact, no resolution could be obtained for the enantiomers of the latter compound, even at a low temperature. Furthermore, for compound **5**, no separation for the ^1H NMR methyl doublet could be seen at room temperature, even at the molar ratio of 2.5. However, at lower temperature ($-20\text{ }^\circ\text{C}$), resolution could be achieved, but $\Delta\Delta\delta$ values were smaller than for compound **2** (0.0063 versus 0.0310 ppm).

Interestingly, even the α -carbonyl enantiotopic protons of *N,N*-diphenylphenylacetamide (**6**), devoid of a carbon stereocenter, could be separated into two doublets in presence of **1**, at $-20\text{ }^\circ\text{C}$ and at 2.5 molar ratio (Table 4).

Table 4.

$\Delta\Delta\delta$ values for mixtures of **1** and **6** (5 mg / mL), at different molar ratios, at room temperature and at $-20\text{ }^\circ\text{C}$.

1 : 6 molar ratio	$\Delta\Delta\delta$ (ppm)	
	(r. t.)	($-20\text{ }^\circ\text{C}$)
0	0 ($\delta = 3.6643$ ppm)	0 ($\delta = 3.6643$ ppm)
0.5	0.0407	0.0518
1.0	0.0497	0.0737
1.5	0.0508	0.0904
2.0	0.0558	0.0927
2.5	0.0565	0.1157

As opposed to **1**, quinine showed to be an inefficient chiral auxiliary for ^1H NMR signal resolution for substrates **2** - **6**. On the contrary, enantiodiscrimination of methyl protons of each enantiomer of 2-phenyl-1-propanol could only be achieved in the presence of quinine. In this case, for both enantiomers, downfield shifts could be observed at room temperature or at $-20\text{ }^\circ\text{C}$ (Table 5).

Table 5.

$\Delta\Delta\delta$ values for mixtures of quinine and 2-phenyl-1-propanol (5 mg / mL) for different molar ratios, at room temperature and at $-20\text{ }^\circ\text{C}$.

quinine : 2-phenyl-1-propanol molar ratio	$\Delta\Delta\delta$ (ppm)	
	(r. t.)	(-20 °C)
0	0 (δ = 1.2552 ppm)	0 (δ = 1.2680 ppm)
0.5	0	0
1.0	0.0013	0.0043
1.5	0.0020	0.0051
2.0	0.0024	0.0066
2.5	0.0030	0.0071

The *R* configuration of the better interacting enantiomer of 2-phenyl-1-propanol could be assigned by comparison of ^1H NMR spectral data of racemic quinine solvates with those for solvates of quinine and an (*R*)-enriched mixture (e.e. 27%) of the same alcohol, prepared by biocatalytic resolution.

Conclusion

The alkaloid salt **1** is an effective chiral discriminating agent for carbonyl and carboxyl compounds **2** – **5**. For compounds **3** and **4** lower $\Delta\delta$ and $\Delta\Delta\delta$ values were observed as compared to those for compound **2**. This seems to be in line with the expected basicity order amide > aldehyde > ketone. Such comparative results point to the importance of the hydrogen bonding between the C-9 hydroxyl group of **1**, and the carbonyl oxygen. Theoretical calculations showed that the π - π interactions are responsible for the higher stability of the diastereomeric pair **1** / (*R*)-**2**.

Acknowledgements

We thank FAPESP, CNPq and CAPES for financial support. We also thank Prof. Dr. Cláudio Francisco Tormena for some previous calculations regarding compound **2**.

Supplementary data

See supplementary data for experimental procedures, spectral data and other files associated to this work.

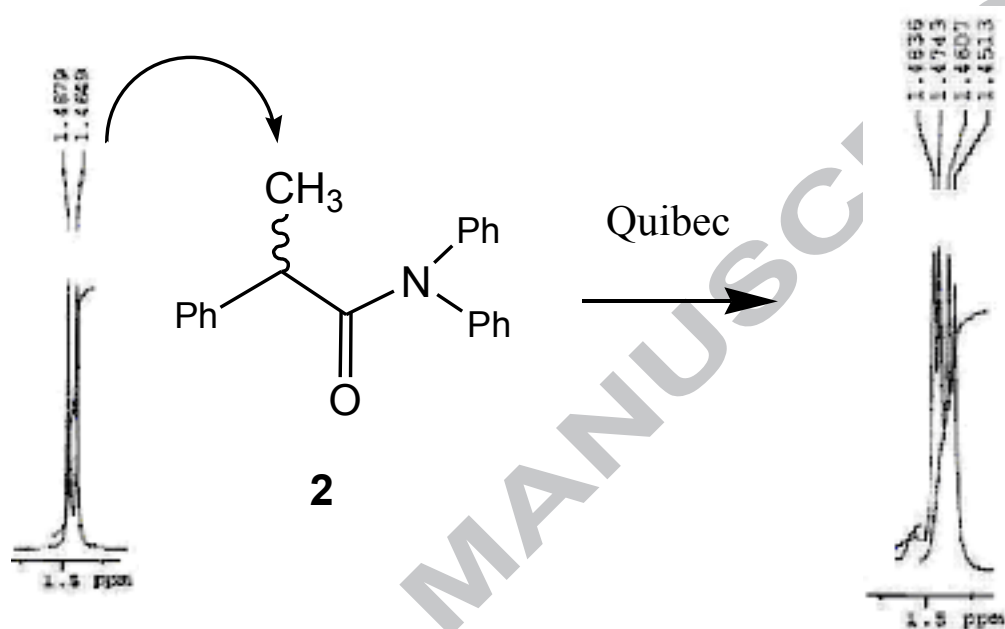
References and Notes

1. Auvil, T. J.; Schafer, A. G.; Mattson, A. E. *Eur. J. Org. Chem.* **2014**, 2633-2646.

2. Tang, Z.; Cun, L. F.; Cui, X.; Mi, A. Q.; Jiang, Y. Z.; Gong, I. Z. *Org. Lett.* **2006**, *8*, 1263-1266.
3. Jones, G. B.; Chapman, B. J. *Synthesis* **1995**, 475-497.
4. Uccello-Barretta, G.; Balzano, F.; Piero Salvadori, P. *Curr. Pharm. Design* **2006**, *12*, 4023-4045.
5. Wenzel, T.J.; Wilcox, J. D. *Chirality* **2003**, *15*, 256-270.
6. Seker, S.; Baris, D.; Arslan, N.; Turgut, Y.; Pirinccioglu, N.; Togrul, M. *Tetrahedron: Asymmetry* **2014**, *25*, 411-417.
7. Schefzick, S.; Lindner, W.; Lipkowitz, K. B.; Jalaie, M. *Chirality* **2000**, *12*, 7-15.
8. Jew, S.; Park, H. *Chem. Commun.* **2009**, 7090-7103.
9. Rodrigues, A.; Wladislaw, B.; Di Vitta, C.; Cardoso-Filho, J. E. P.; Marzorati, L.; Bueno, M. A.; Olivato, P. R. *Tetrahedron Lett.* **2010**, *51*, 5344-5348.
10. Goldberg, Y. "Phase Transfer Catalysis: selected problems and applications", chap. 6, 293-338, **1992**, Gordon and Breach Publishers.
11. Marzorati, L.; Fejfar J. L.; Tormena, C. F.; Di Vitta, C. *Tetrahedron: Asymmetry* **2012**, *23*, 748-753.
12. Rudzinska, E.; Berlicki, L.; Kafarski, P.; Lammerhofer, M.; Mucha, A. *Tetrahedron: Asymmetry* **2009**, *20*, 2709-2714.
13. Gorecki, L.; Berlick, L.; Mucha, A.; Kafarski, P.; Slepokura, K.; Rudzinska-Szostak, E. *Chirality* **2012**, *24*, 318-328.
14. Uccello-Barretta, G.; Vanni, L.; Berni, M. G.; Balzano, F. *Chirality* **2011**, *23*, 417-423.
15. Uccello-Barretta, G.; Balzano, F.; Quintavalli, C.; Salvadori P. *J. Org. Chem.* **2000**, *65*, 3596-3602.
16. Gaussian 09, Revision D.01, Frisch, M. J.; Trucks, G. W.; Schlegel, H. B.; Scuseria, G. E.; Robb, M. A.; Cheeseman, J. R.; Scalmani, G.; Barone, V.; Mennucci, B.; Petersson, G. A.; Nakatsuji, H.; Caricato, M.; Li, X.; Hratchian, H. P.; Izmaylov, A. F.; Bloino, J.; Zheng, G.; Sonnenberg, J. L.; Hada, M.; Ehara, M.; Toyota, K.; Fukuda, R.; Hasegawa, J.; Ishida, M.; Nakajima, T.; Honda, Y.; Kitao, O.; Nakai, H.; Vreven, T.; Montgomery, J. A., Jr.; Peralta, J. E.; Ogliaro, F.; Bearpark, M.; Heyd, J. J.; Brothers, E.; Kudin, K. N.; Staroverov, V. N.; Kobayashi, R.; Normand, J.; Raghavachari, K.; Rendell, A.; Burant, J. C.; Iyengar, S. S.; Tomasi, J.; Cossi,

- M.; Rega, N.; Millam, J. M.; Klene, M.; Knox, J. E.; Cross, J. B.; Bakken, V.; Adamo, C.; Jaramillo, J.; Gomperts, R.; Stratmann, R. E.; Yazyev, O.; Austin, A. J.; Cammi, R.; Pomelli, C.; Ochterski, J. W.; Martin, R. L.; Morokuma, K.; Zakrzewski, V. G.; Voth, G. A.; Salvador, P.; Dannenberg, J. J.; Dapprich, S.; Daniels, A. D.; Farkas, Ö.; Foresman, J. B.; Ortiz, J. V.; Cioslowski, J.; Fox, D. J. Gaussian, Inc., Wallingford CT, **2009**.
17. Grimme, S.; Antony, J.; Ehrlich S.; Krieg, H. *J. Chem. Phys.* **2010**, *132*, 154104.
18. Tomasi, J.; Mennucci, B.; Cammi, R. *Chem. Rev.* **2005**, *105*, 2999–3093.
19. Simon, S.; Duran, M.; Dannenberg, J. J. *J. Chem. Phys.* **1996**, *105*, 11024–11031.

Graphical abstract



Highlights

Chiral discrimination of carbonyl group containing compounds was achieved using Quibec.

Basic amides are better discriminated than ketones and aldehydes.

Chiral discrimination relies on π - π stacking and hydrogen bonding interactions.